

This article was downloaded by:

On: 25 January 2011

Access details: *Access Details: Free Access*

Publisher *Taylor & Francis*

Informa Ltd Registered in England and Wales Registered Number: 1072954 Registered office: Mortimer House, 37-41 Mortimer Street, London W1T 3JH, UK



Separation Science and Technology

Publication details, including instructions for authors and subscription information:

<http://www.informaworld.com/smpp/title~content=t713708471>

Removal of Acetic Acid by Adsorption from an Ethylene Recycle Stream in the Ethylene-Vinyl Acetate Copolymerization Process

Antonio De Lucas^a; G. Ovejero^b; A. Sánchez^b; Antonio Durán^c

^a DEPARTMENT OF CHEMICAL ENGINEERING, UNIVERSITY OF CASTILLA-LA MANCHA

(UCLM), CAMPUS UNIVERSITARIO, CIUDAD REAL, SPAIN ^b DEPARTMENT OF CHEMICAL

ENGINEERING, UNIVERSITY COMPLUTENSE OF MADRID (UCM), MADRID, SPAIN ^c

DEPARTMENT OF CHEMICAL ENGINEERING, UNIVERSITY OF CASTILLA-LA MANCHA
(UCLM), CAMPUS UNIVERSITARIO, CIUDAD REAL, SPAIN

Online publication date: 22 February 1999

To cite this Article De Lucas, Antonio , Ovejero, G., Sánchez, A. and Durán, Antonio(1999) 'Removal of Acetic Acid by Adsorption from an Ethylene Recycle Stream in the Ethylene-Vinyl Acetate Copolymerization Process', Separation Science and Technology, 34: 3, 525 – 543

To link to this Article: DOI: 10.1081/SS-100100664

URL: <http://dx.doi.org/10.1081/SS-100100664>

PLEASE SCROLL DOWN FOR ARTICLE

Full terms and conditions of use: <http://www.informaworld.com/terms-and-conditions-of-access.pdf>

This article may be used for research, teaching and private study purposes. Any substantial or systematic reproduction, re-distribution, re-selling, loan or sub-licensing, systematic supply or distribution in any form to anyone is expressly forbidden.

The publisher does not give any warranty express or implied or make any representation that the contents will be complete or accurate or up to date. The accuracy of any instructions, formulae and drug doses should be independently verified with primary sources. The publisher shall not be liable for any loss, actions, claims, proceedings, demand or costs or damages whatsoever or howsoever caused arising directly or indirectly in connection with or arising out of the use of this material.

Removal of Acetic Acid by Adsorption from an Ethylene Recycle Stream in the Ethylene–Vinyl Acetate Copolymerization Process

ANTONIO DE LUCAS

DEPARTMENT OF CHEMICAL ENGINEERING
UNIVERSITY OF CASTILLA-LA MANCHA (UCLM)
CAMPUS UNIVERSITARIO
S/N. 13071 CIUDAD REAL, SPAIN

G. OVEJERO AND A. SÁNCHEZ

DEPARTMENT OF CHEMICAL ENGINEERING
UNIVERSITY COMPLUTENSE OF MADRID (UCM)
MADRID, SPAIN

ANTONIO DURÁN*

DEPARTMENT OF CHEMICAL ENGINEERING
UNIVERSITY OF CASTILLA-LA MANCHA (UCLM)
CAMPUS UNIVERSITARIO
S/N. 13071, CUIDAD REAL, SPAIN

ABSTRACT

The quality of EVA copolymers (ethylene and vinyl acetate copolymers) depends on the impurities in the feed. The removal of acetic acid, formed due to the partial degradation of the EVA copolymer, by adsorption from the recycle ethylene stream has been studied. Activated carbon proved to be useful for this purpose due to its high adsorption capacity and selectivity to acetic acid and its easy and complete regeneration. Adsorption isotherms and breakthrough curves of ethylene, acetic acid, and vinyl acetate, and binary acetic acid–vinyl acetate mixtures have been obtained at 293 K. Mass transfer and pore diffusion coefficients have been determined using two adsorption models. These data have allowed the design of an adsorption installation for the improvement of quality of EVA copolymer.

Key Words. Adsorption; Kinetic coefficients; Removal

* To whom correspondence should be addressed. Telephone: 34-26-295300, ext. 3814. FAX: 34-26-295318. E-mail: aduran@inqu-cr.uclm.es

INTRODUCTION

The discovery of new polymeric materials with special properties has led to the substitution of traditional materials in many industrial applications and the development of new commercial products (1).

Ethylene and vinyl acetate copolymers (EVA) are very important industrial polymers with a large number of applications. Thermal and chemical stability, resistance to aging, and thermal distortion are remarkable properties of these polymers (2).

EVA copolymers are industrially obtained from ethylene and vinyl acetate copolymerization at high pressure (1500–2000 atm) and temperature (150–200°C). They are currently produced at Repsol Química (Ciudad Real, Spain) with a production of 25.000 tonne/year (3). Ethylene is compressed in two stages before being fed to the reactor. Vinyl acetate is added to the feed before it enters the second compression stage. The product leaving the reactor is decompressed (300 atm) and conducted to a high-pressure separator which produces a liquid stream and a gaseous stream which is recycled back to the second compression stage. In order to improve the final quality of the product, the removal of acetic acid formed by the partial degradation of the copolymer from the recycle ethylene stream has been proposed.

In previous work the removal of acetic acid by absorption with different solvents was investigated (4). Mass transfer coefficients needed for absorber simulation and design were obtained. However, the absorber was imperfectly simulated by the use of a nonequilibrium model which reproduced the experimental results with deviations up to 20%.

On the other hand, the increasing importance of adsorption as a separation operation in fluid mixtures (5–8) has motivated the development of a great number of solid adsorbents, both natural and synthetic. Their typical properties are high adsorption capacity and selectivity, easy regeneration, high mechanical resistance, and low price. Industrial application of adsorbents depends not only on their structure but also on the polarity on their surface (9).

The aim of this work is to study the adsorption of ethylene, vinyl acetate, acetic acid, and their mixtures by evaluating the kinetic parameters in order to design an installation able to improve the final quality of the EVA copolymer. Two adsorption models have been used to obtain the kinetic parameters.

EXPERIMENTAL

The experimental adsorption setup is shown in Fig. 1. A Pyrex column attached to a external heat exchanger holds the adsorbent bed. The system allows the measurement of pressure and temperature of the gas stream entering



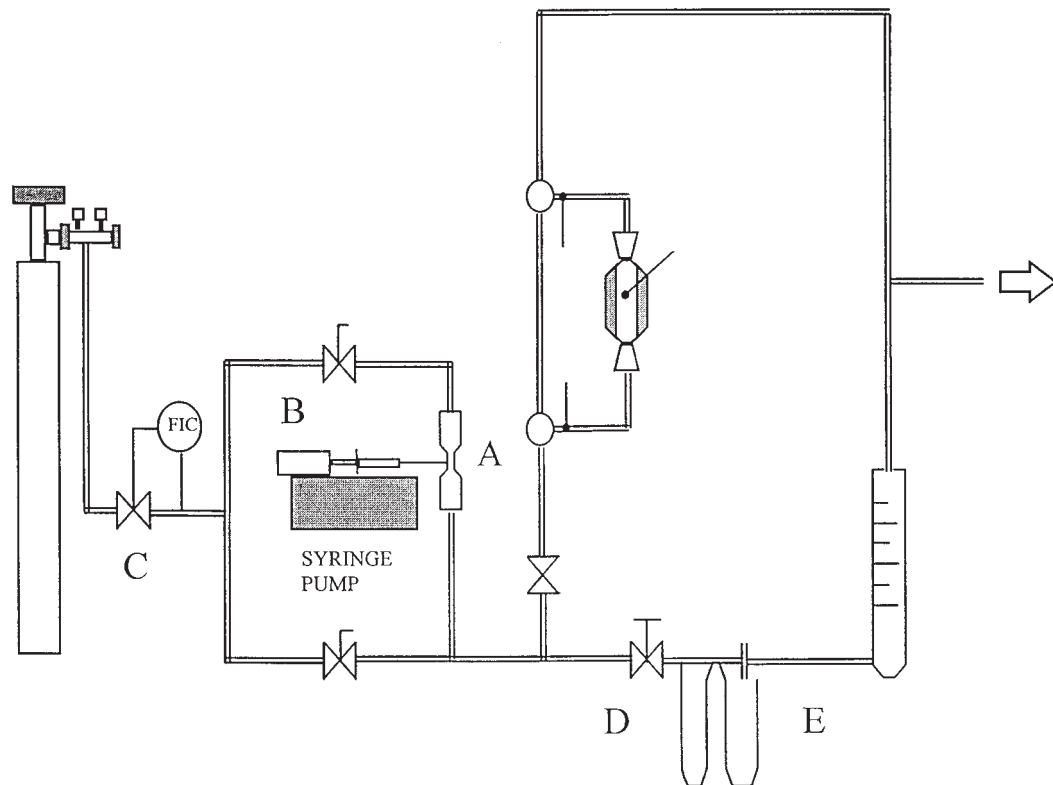


FIG. 1 Adsorption experimental setup.

and leaving the column. An additional heat source allows regeneration of the adsorbents.

Gaseous mixtures are produced by vaporizing acetic acid in a glass mixer (A) while helium or ethylene is flowing. A by-pass and a valve system allow the circulation of a fraction of the whole gas flow through the mixer. Liquid acetic acid is fed to the mixer using a syringe pump (B). A mass flow indicator-regulator (C) controls the total flow rate (up to 100 normal conditions L/min). When higher flow rates are needed, the regulation and measurement of the flow is made by means of a needle valve (D) and an orifice meter (E). Gas composition is analyzed by gas chromatography.

The main characteristics of the activated carbon and the adsorption bed are summarized in Table 1.

The amount of adsorbate retained in the adsorbent (n_i , mol/g) is calculated from the breakthrough curves:

$$n_i = \frac{VP_T}{RT} \left(y_{i,1} t_F - \int_{t_R}^{t_F} y_{i,2} dt \right) \frac{1}{W_s} \quad (1)$$



TABLE 1
Characteristics of Activated Carbon and Adsorption Bed

Activated carbon:	
Average diameter (mm)	1.45
Apparent density (g/cm ³)	0.75
Skeletal density (g/cm ³)	1.79
Pore volume (cm ³ /g)	0.77
Porosity	0.58
Surface area (m ² /g)	1997
Average mesopore radius (Å)	260
Adsorption bed:	
Density (g/cm ³)	0.34
Porosity	0.51

where V is the gas flow rate (L/min); P_T (atm) is the pressure inside the bed; $y_{i,1}$ and $y_{i,2}$ are the molar fraction of Component i at the inlet and outlet of the bed, respectively; t_R (minutes) is the breakthrough time; t_F (minutes) represents the time at which the concentrations at the inlet and outlet the bed are equal; and W_s (g) is the amount of adsorbent.

RESULTS AND DISCUSSION

Adsorbent Selection and Regeneration

Several adsorbents were selected by taking into consideration that they should allow the diffusion of acetic acid and favor the formation of hydrogen bridges without inducing dipoles so that adsorption is selective. The fact that vinyl acetate may interfere during the adsorption process and during the regeneration of the adsorbent should also be considered when applying this process to industrial operations.

Thus, several zeolites of adequate pore size (5A, 13X, YNa, and silicalite) and high affinity to polar substances and activated carbon with a high affinity to organic compounds were preselected.

A first set of experiments was carried out to determine the adsorption capacity and selectivity of each adsorbent. Results are summarized in Table 2. A longer breakthrough time can be observed for activated carbon.

Several mixture adsorption experiments (ethylene-acetic acid, ethylene-vinyl acetate, and ethylene-acetic acid-vinyl acetate) were made on virgin activated carbon, and additional ethylene-acetic acid experiments were performed on carbon previously saturated with vinyl acetate.

Figure 2 shows breakthrough curves of ethylene-acetic acid and ethylene-vinyl acetate on activated carbon. Breakthrough time for acetic acid is



TABLE 2
Selection of the Adsorbent (ethylene-acetic acid).
 M_1 (feed mass flow) = 49.7 g/h. T = 293 K

Adsorbent	W_s (g)	$y_1 \times 10^2$	t_R (h) ^a
Zeolite 5A	5.98	1.03	0.0
Zeolite YNa	3.10	1.68	0.2
Zeolite 13X	6.49	0.92	0.2
Activated carbon	4.66	1.02	1.4
Silicalite	5.31	1.07	0.0

^a t_R = breakthrough time at $Y/Y_0 = 0.5$.

nearly double that for vinyl acetate, which is indicative of the higher adsorption capacity of activated carbon for the former. However, the shape of both curves is quite similar, suggesting similar adsorption kinetic behavior.

Since both compounds are present in the industrial recycle stream when EVA copolymers are obtained, it is important to know whether or not acetic acid displaces vinyl acetate during the simultaneous adsorption of both substances on activated carbon. It can be seen from the experiments (shown in Fig. 3a) that the carbon initially adsorbs both compounds, although saturation in vinyl acetate is quickly achieved. The concentration of vinyl acetate reaches a maximum, then decreases slowly to equal the initial entrance value because it is displaced by acetic acid.

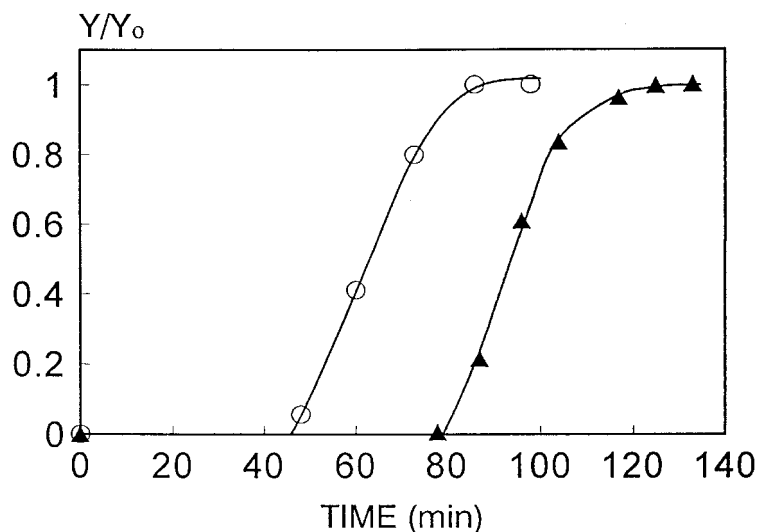
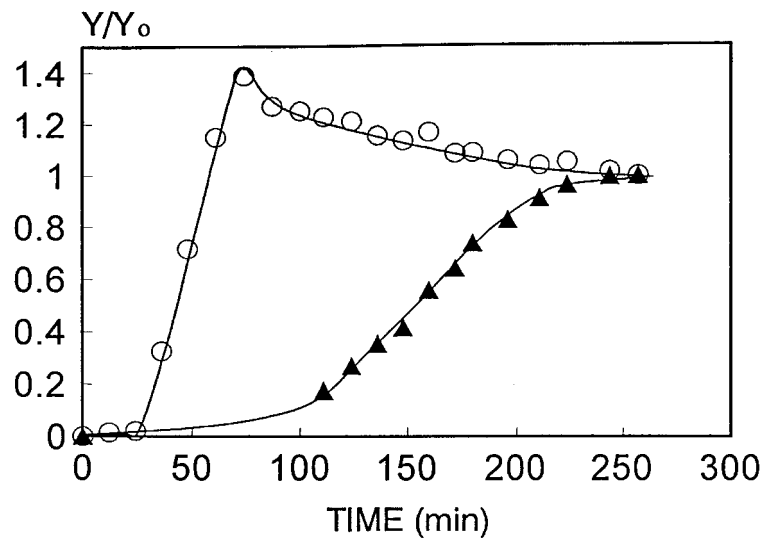
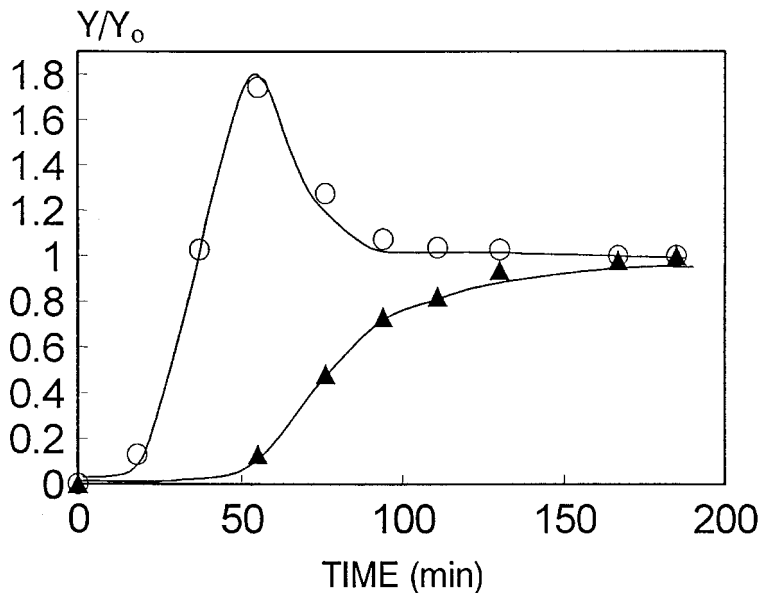


FIG. 2 Binary mixture adsorption on virgin activated carbon. (○) $W_s = 4.62$ g; $M_1 = 47.90$ g/h; $Y_1 = 1.707 \times 10^{-2}$; ethylene-vinyl acetate system. (▲) $W_s = 4.18$ g; $M_1 = 50.0$ g/h; $Y_1 = 0.819 \times 10^{-2}$; ethylene-acetic acid system.





a)



b)

FIG. 3 a): Ethylene-acetic acid-vinyl acetate adsorption on virgin activated carbon. $W_s = 4.18$ g; $M_1 = 50.0$ g/h; $Y_{\text{Ac. Acid } 1} = 0.481 \times 10^{-2}$; $Y_{\text{vinyl ac. } 1} = 1.034 \times 10^{-2}$. (○) Vinyl acetate; (▲) acetic acid. b): Adsorption of ethylene-acetic acid from an industrial plant on virgin activated carbon. $W_s = 4.18$ g; $M_1 = 50.0$ g/h; $Y_{\text{Ac. Acid } 1} = 1.425 \times 10^{-2}$; $Y_{\text{vinyl ac. } 1} = 0.070 \times 10^{-2}$. (○) Vinyl acetate; (▲) acetic acid.



Furthermore, the shape of the breakthrough curve for vinyl acetate is similar to that found for pure component adsorption; this means that acetic acid is not affecting the kinetics of the process. On the contrary, acetic acid adsorption is slower as a pure component. This can be explained if vinyl acetate restricts the diffusion of acetic acid molecules to the adsorption sites and/or if vinyl acetate molecules already adsorbed decrease acetic acid adsorption velocity.

The latter assumption can be confirmed by comparing the experimental breakthrough curve in Fig. 3 with that obtained from the adsorption of ethylene-acetic acid on activated carbon previously saturated with vinyl acetate (Fig. 4).

The shape of both curves is similar, confirming that vinyl acetate molecules produce a decrease in adsorption velocity of acetic acid.

As this adsorbent is intended to be used for the industrial upgrading of EVA copolymers, breakthrough curves of ethylene-acetic acid obtained in an industrial plant on virgin carbon were performed (Fig. 3b). Activated carbon maintains the affinity to acetic acid, so it is adequate for use in industrial application.

Finally, it was shown that activated carbon, once regenerated at 200°C under nitrogen flow for 12 hours, showed the same behavior in adsorption experiments.

Optimum regeneration conditions were selected from regeneration tests (Table 3). There is a minimum in the treatment intensity at $T = 498$ K and $t = 1.62$ hours. Additional experiments with adsorbent regenerated for 12 hours confirmed the complete regeneration of the carbon under these conditions.

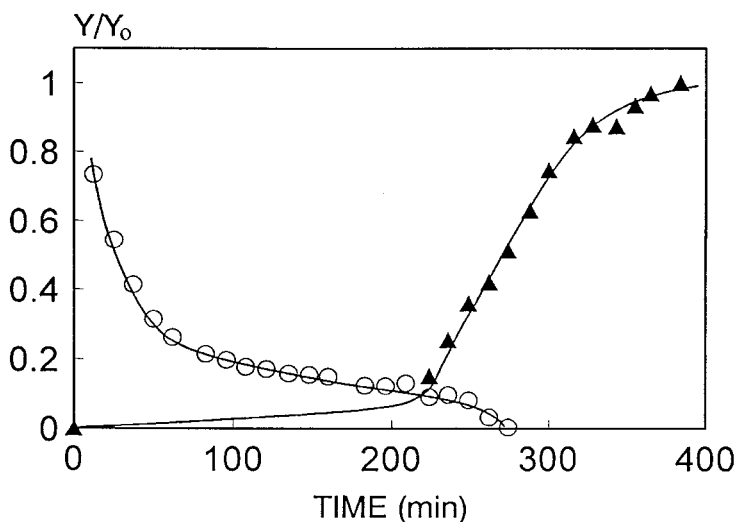


FIG. 4 Ethylene-acetic acid adsorption on activated carbon saturated with vinyl acetate. $W_s = 4.18$ g; $M_1 = 50.0$ g/h; $Y_1 = 0.342 \times 10^{-2}$; (○) vinyl acetate; (▲) acetic acid.



TABLE 3
Regeneration Tests for Activated Carbon
($V_{N_2} = 27.5$ normal conditions L/h, $W_s = 3$ g)

t_{\min} (h)	T (K)	I (K·h)
4.70	423	1988
3.55	448	1590
2.17	473	1026
1.62	498	807
1.55	523	811

We conclude that activated carbon has a high adsorption capacity and selectivity to acetic acid and is adequate for removing this acid from gaseous mixtures with vinyl acetate and ethylene. The adsorption process has thus proved to be feasible, but adsorption and kinetic data are needed in order to design industrial equipment.

Pure Compound Adsorption Data

Equilibrium adsorption data for pure acetic acid, vinyl acetate, and ethylene were determined from breakthrough curves in a fixed bed (10). The calculation is based on the assumption that the adsorbent is saturated when the adsorbate concentration in the outer stream is constant and equals the concentration in the inner stream. Helium was selected as the inert gas in order to obtain gaseous mixtures with different concentrations without affecting the adsorption process (3).

The adsorption data were adjusted to the Langmuir, Freundlich, and Prausnitz isotherms. Equation parameters and average deviation obtained for each isotherm are summarized in Table 4.

Two adsorption models have been applied in this work in order to obtain kinetic parameters for pure compounds. Basically, both models are characterized by the mass balances inside and outside the adsorbent and by equilibrium adsorption data.

Mathematical Models for Pure Compound Adsorption

Adsorption Model with Overall Mass Transfer Coefficients. During the development of this model (11), several assumptions are formulated:

- The operation is isothermal
- The adsorbent particles are spherical
- The adsorption velocity is much higher than the diffusion velocity



TABLE 4
 Adjustment Parameters for Equilibrium Data of Pure Compounds

Compound	Langmuir: $n_i = Ap_i/B + p_i$	Freundlich: $n_i = Cp_i^D$	Prausnitz: $\frac{1}{n_i} = \frac{1}{Ep_i} + \frac{1}{Fp_i^G}$
Ethylene	$A = 0.0388$ $B = 0.0411$ $\delta_M = 2.0\%$	$C = 0.0428$ $D = 0.753$ $\delta_M = 2.7\%$	$E = 0.0388$ $F = 0.945$ $G = 0.001$ $\delta_M = 2.0\%$
Acetic acid	$A = 18.287$ $B = 1.529$ $\delta_M = 2.2\%$	$C = 7.762$ $D = 0.173$ $\delta_M = 2.7\%$	$E = 27.404$ $F = 10.146$ $G = 0.0683$ $\delta_M = 1.7\%$
Vinyl acetate	$A = 8.365$ $B = 1.518$ $\delta_M = 2.7\%$	$C = 3.340$ $D = 0.202$ $\delta_M = 7.2\%$	$E = 6.589$ $F = 6.680$ $G = -0.085$ $\delta_M = 2.2\%$

Furthermore, axial dispersion and adsorbate accumulation in the gas occupying adsorbent pores can be considered negligible. The mass balance for the transferred component in the gas phase in a differential element of the bed can be formulated as

$$v \frac{\partial c_i}{\partial z} + \epsilon_L \frac{\partial c_i}{\partial t} + \rho_L \frac{\partial n_i}{\partial t} = 0 \quad (2)$$

where v (m/s) is the average gas velocity referred to the empty bed, c_i (mol/m³) is the concentration of Adsorbate i in the gas phase, n_i (mol/kg) is the concentration in the solid phase, t (seconds) is the time, z (m) is the distance between a bed point and the bed entrance, ρ_L (kg/m³) is the bed density, and ϵ_L is the bed porosity.

On the other hand, adsorbate accumulation in the solid phase can be expressed as a function of the flow of the component that is dispersed into the particle as

$$\rho_p \frac{\partial n_i}{\partial t} = \frac{3\epsilon_p}{R} D_{p,j} \left(\frac{\partial c_{p,i}}{\partial r} \right)_{r=R} \quad (3)$$

where ρ_p (kg/m³) is the particle density, $c_{p,i}$ (m²/s) is the intraparticle diffusion coefficient, and R (m) is the average ratio of carbon particles.

Assuming a fast adsorption phenomenon, the concentration of component



in the gas filling the pores can be related to the concentration in the solid phase by means of the equilibrium isotherm

$$n_i = \phi(c_{p,i}) \quad (4)$$

Furthermore, the concentration of adsorbate inside and outside the pores is related to the film mass transfer coefficient $K_{e,i}$ by

$$K_{e,i}[c_i - c_{p,i}^s] = \varepsilon_p D_{p,i} \left(\frac{\partial c_{p,i}}{\partial r} \right)_{r=R} \quad (5)$$

where $c_{p,i}^s$ is the gas adsorbate concentration at the particle surface.

Resolution of this system of equations with adequate boundary conditions would lead to the theoretical breakthrough curves. A new internal mass transfer coefficient ($K_{l,i}$) is introduced in order to simplify the calculations:

$$K_{l,i} = \frac{D_{p,i}}{\delta} \quad (6)$$

where δ (m) is the average diffusion path of adsorbate molecules inside the carbon, which can be estimated as $R/4$ (11).

So, Eqs. (3) and (5) are changed into

$$\rho_p \frac{\partial n_i}{\partial t} = \frac{3K_e}{R} (c_i - c_{p,i}^s) = \frac{3K_{l,i}}{R} (c_{p,i}^s - c_i^*) = \frac{3K_i}{R} (c_i - c_i^*) \quad (7)$$

where c_i^* is the gas concentration of Component i in equilibrium with the solid-phase concentration, and K_i is the overall mass transfer coefficient:

$$\frac{1}{K_i} = \frac{1}{K_{e,i}} + \frac{\delta}{D_{p,i}} \quad (8)$$

The boundary conditions are

$$t = 0; \quad 0 < z < L; \quad c_i = 0; \quad n_i = 0 \quad (9)$$

$$t \geq 0; \quad z = 0; \quad c_i = c_0 \quad (10)$$

where L is the bed length.

The resolution of this model has been carried out by using a finite difference method.

Adsorption Model with Pore Diffusion. Initial assumptions are the same as in the previous model, but in this case axial dispersion and adsorbate

DEKKER, INC.
270 Madison Avenue, New York, New York 10016



accumulation in the gas-occupying adsorbent pores are also considered (12). The general mass equation outside the adsorbent is reduced to

$$\frac{\partial c_i}{\partial t} = D_{L,i} \frac{\partial^2 c_i}{\partial z^2} - u \frac{\partial c_i}{\partial z} - \frac{3}{R} \frac{(1 - \varepsilon_L)}{\varepsilon_L} \left(\varepsilon_p D_{p,i} \frac{\partial c_{p,i}}{\partial r} \right)_{r=\bar{R}} \quad (11)$$

where u (m^2/s) is the velocity of the fluid phase through the bed, referred to the free transversal section, and $D_{L,i}$ (m^2/s) is the axial dispersion coefficient.

The mass equation inside the adsorbent is

$$\rho_p \frac{\partial n_i}{\partial t} + \varepsilon_p \frac{\partial c_{p,i}}{\partial r} = \frac{1}{r^2} \frac{\partial}{\partial r} \left(r^2 D_{p,i} \varepsilon_p \frac{\partial c_{p,i}}{\partial r} \right) \quad (12)$$

Equations (4), (11), and (12) are the mathematical model for simulation. Initial and contour conditions are as follows.

Mass balance outside the adsorbent:

$$\text{Initial condition: } t = 0; \quad 0 < z < L; \quad c_i = 0 \quad (13)$$

Contour conditions:

$$t > 0; \quad D_{L,i} \left(\frac{\partial c_i}{\partial z} \right)_{z=0} = -u(c_{i,z=0-} - c_{i,z=0+}) \quad (\text{bed entry}) \quad (14)$$

$$t > 0; \quad z = L; \quad \frac{\partial c_i}{\partial z} = 0 \quad (\text{outlet the bed}) \quad (15)$$

Mass balance inside the adsorbent:

$$\text{Initial condition: } t = 0; \quad 0 < r < R; \quad c = c_0; \quad n = n_0 \quad (16)$$

Contour conditions:

$$t > 0; \quad r = 0; \quad \frac{\partial c_{p,i}}{\partial r} = 0; \quad \frac{\partial n_i}{\partial r} = 0 \quad (\text{spherical geometry}) \quad (17)$$

$$K_{e,i} [c_i - c_{p,i}^s] = \varepsilon_p D_{p,i} \left(\frac{\partial c_{p,i}}{\partial r} \right)_{r=\bar{R}} \quad (\text{external surface}) \quad (18)$$

The resolution of this model has been carried out using the orthogonal location method.

Determination of the Overall Mass Transfer Coefficients of Pure Compounds

In order to determine the overall mass transfer coefficients of pure ethylene, acetic acid, and vinyl acetate, experimental breakthrough curves were

270 Madison Avenue, New York, New York 10016



fitted to the proposed model. Coefficients minimizing deviations between experimental and theoretical values were selected. The results are summarized in Table 5.

It can be concluded that neither adsorbate concentration nor adsorbent amount have an effect on the coefficient K in the range of concentrations studied; concentrations are low and surface diffusivity does not significantly contribute to the overall diffusional process. However, a slight increase in the gas flow rate produces a corresponding increase of K , which is a logical result of the increased resistance to mass transfer outside the particles.

The results of the simulation are in good agreement with experimental data for ethylene, but they are poorer for the adsorptions of acid acetic and vinyl acetate. An example of experimental and model adjustment data is shown in Fig. 5.

Determination of Pore Diffusion Coefficients for Pure Compounds

A comparison of experimental kinetic curves and those predicted by the model allows determination of the diffusion coefficient by minimizing deviations. The external mass and axial dispersion coefficients were calculated from fluid-dynamic experimental conditions and physical properties using the equations proposed by Wakao and Funazkri (13) and Edwards and Richardson (14), respectively.

Diffusion coefficients and pore diffusion model parameters for helium–ethylene, helium–acetic acid, and helium–vinyl acetate are reported in Table 5.

Mean deviations of the fittings obtained with this second model are lower than with the first one, and pore diffusion coefficients can be averaged in the range studied to 1.7×10^{-6} , 8.4×10^{-7} , and 6.6×10^{-7} (m^2/s) for ethylene, acetic acid, and vinyl acetate, respectively. Examples of the correlation between experimental and modeled data and the model are shown in Fig. 5.

On the other hand, a comparison between the pore diffusivity with molecular and Knudsen diffusivity has been made and the tortuosity has been deduced. The carbon has a pore size distribution characterized by a major number of mesopores (20–500 Å) (15). Therefore, an average pore size of 260 Å (Table 1) has been estimated for the calculation of Knudsen diffusivity.

The correlation of Fuller, Schettler, and Giddings (16) has been used to calculate the molecular diffusivities:

$$D_{AB} = \frac{10^{-3} T^{1.75} \left[\left(\frac{M_A + M_B}{M_A + M_B} \right) \right]^{1/2}}{p [(\Sigma V_A)^{1/3} + (\Sigma V_B)^{1/3}]^2} \quad (19)$$



TABLE 5
Kinetic Coefficients and Comparison of Intraparticle Diffusion Coefficients Obtained with the Two Adsorption Models

System	$V \times 10^2$ (m ³ /h)	W_s (g)	Overall mass transfer model				Pore diffusion model				
			$y_{i,1} \times 10^2$	$K_i \times 10^3$ (m/s)	δ_M (%)	$D_i \times 10^6$ (m ² /s)	$D_{p,i} \times 10^6$ (m ² /s)	$K_i \times 10^3$ (m/s)	$D_L \cdot 10^5$ (m ² /s)	δ_M (%)	$D_i \times 10^6$ (m ² /s)
Helium-ethylene	7.17	20.01	1.48	6.99	4.5	1.0	1.7	10.07	4.53	3.1	
	3.94	20.01	1.47	2.81	3.0		1.0	8.97	3.81	5.6	
	7.09	20.01	0.99	6.78	3.4		2.0	10.03	4.51	2.1	
	3.76	20.01	1.00	4.26	4.5		2.2	9.06	3.87	4.2	1.7
	7.19	10.02	1.47	5.57	7.7		1.5	10.07	4.53	3.4	
	3.88	10.02	1.53	5.10	3.9		1.8	9.06	3.86	6.7	
	7.14	10.02	0.99	6.18	2.7		1.7	10.06	4.53	4.7	
	3.85	10.02	1.00	4.77	1.5		1.8	9.04	3.86	6.3	
Helium-acetic acid	8.91	8.02	1.52	3.84	14	0.48	1.3	8.67	4.56	7.1	
	4.55	8.02	1.44	2.76	9		0.7	7.53	3.33	15.2	
	8.79	8.02	0.95	3.52	16		1.1	8.64	4.52	4.5	
	4.42	8.02	0.92	1.68	10		0.7	7.54	3.32	6.3	0.84
	8.80	4.03	1.54	2.96	14		0.7	8.62	4.52	6.0	
	4.34	4.03	1.49	1.50	13		0.5	7.52	3.31	4.8	
	8.71	4.03	0.94	3.21	13		1.0	8.69	4.51	5.9	
	4.29	4.03	0.97	1.17	20		0.7	7.47	3.28	12.1	
Helium-vinyl acetate	9.02	8.02	1.49	3.05	11	0.43	0.7	7.55	4.38	2.2	
	4.59	8.02	1.47	1.66	13		0.5	6.59	3.01	10.1	
	8.93	8.02	1.03	3.22	14		1.0	7.54	4.35	7.8	
	4.48	8.02	1.03	1.97	19		0.7	6.58	3.01	8.5	0.66
	9.05	4.03	1.50	2.93	12		0.7	7.53	4.39	4.5	
	4.66	4.03	1.49	1.26	13		0.5	6.51	2.99	9.7	
	8.94	4.03	1.05	2.46	12		0.7	7.49	4.35	6.1	
	4.68	4.03	1.03	1.71	12		0.5	6.55	3.01	9.1	



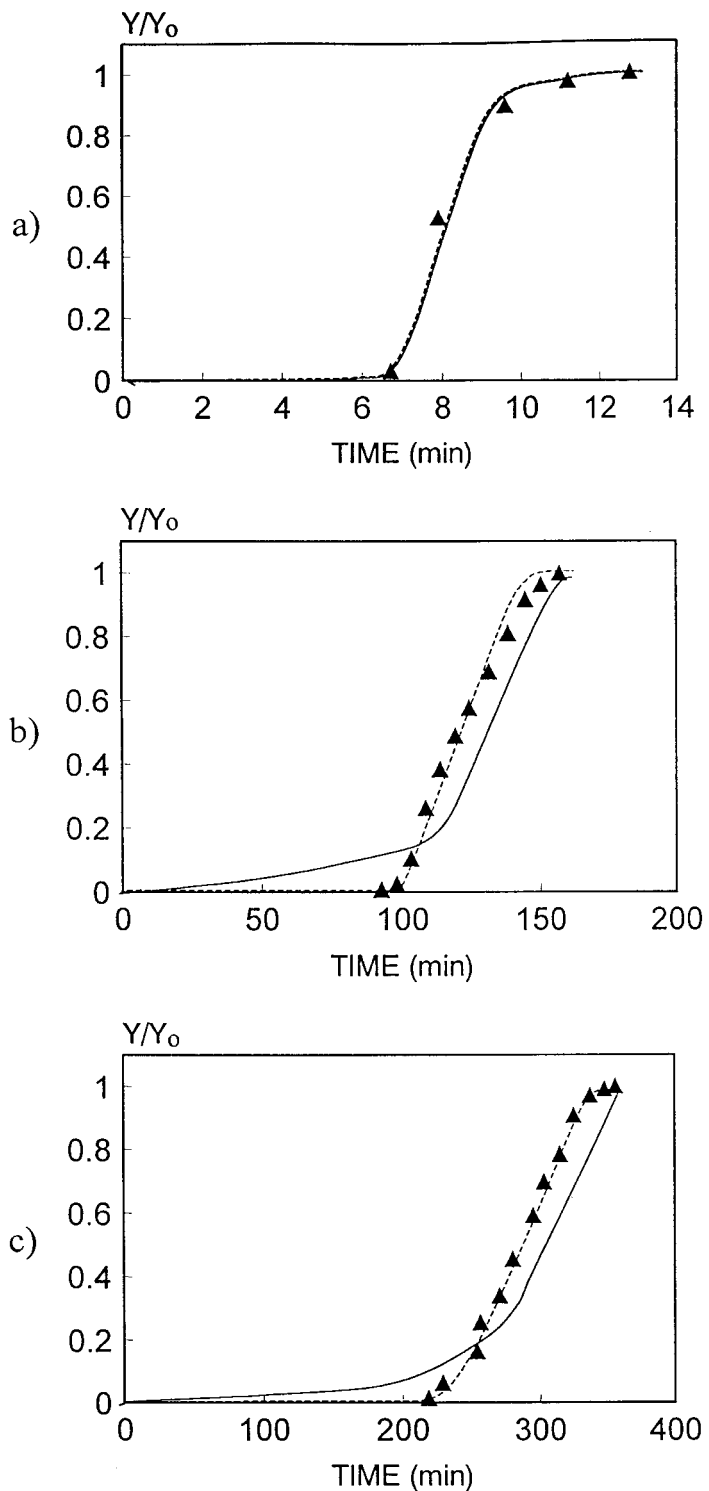


FIG. 5 Pure compound adsorption kinetics. Adsorption model with overall mass transfer coefficients (—) and adsorption model with pore diffusion (---). a): Helium-ethylene ($V = 7.17 \times 10^{-2} \text{ m}^3/\text{h}$; $W_s = 20.01 \text{ g}$). b): Helium-acetic acid ($V = 4.42 \times 10^{-2} \text{ m}^3/\text{h}$; $W_s = 8.02 \text{ g}$). c): Helium-vinyl acetate ($V = 4.48 \times 10^{-2} \text{ m}^3/\text{h}$; $W_s = 8.02 \text{ g}$).



Knudsen diffusivity was estimated from

$$D_K = 9700 \left(\frac{T}{M} \right)^{1/2} \bar{r} \quad (20)$$

Tortuosity comes from

$$\frac{1}{D_p} = \frac{\tau}{\varepsilon} \left(\frac{1}{D_K} + \frac{1}{D_{AB}} \right) \quad (21)$$

Tortuosity values between 2.4 and 3.4 were found (Table 6).

Comparison of Adsorption Models

The model of adsorption with pore diffusion is more complex, but better results are obtained. In order to compare both models, pore diffusion coefficients were calculated from overall mass transfer coefficients by using Eq. (11). $K_{e,i}$ is calculated from the Wakao and Funazkri equation (13). The results reported in Table 5 show diffusion coefficients of the same order of magnitude with both models. The lower values found using the overall mass transfer model are probably due to the assumption of ideal homogeneous spherical particles with an average diffusion path of $R/4$, influences the calculation of the coefficient in Eq. (11).

The results are considered satisfactory enough with both models, so a study of binary adsorption kinetics has been performed with the overall mass coefficient model due to its simplicity.

Binary Mixture Adsorption Data

Equilibrium adsorption data of the helium–acetic acid–vinyl acetate mixture were obtained from experimental breakthrough curves as was previously done for pure compounds (9). Separate adsorption isotherms of acetic acid and vinyl acetate obtained at different molar ratios in the mixture are shown in Fig. 6 and compared with pure compound data.

A decrease in the adsorption capacities of acetic acid and vinyl acetate is observed when they are compared with pure compound adsorption data; this effect is greater for the latter because of the higher affinity of activated carbon for acetic acid.

The equilibrium data have been adjusted to the following equations (17):

$$n_A = \frac{58.32 p_A^{1.648}}{1 + 6.949 p_A^{1.506} + 0.914 p_v^{1.467}} \quad (22)$$

$$n_V = \frac{10.66 p_v^{1.104}}{1 + 24.97 p_A^{0.512} + 2.231 p_v^{1.042}} \quad (23)$$



TABLE 6
Estimation of Tortuosity

System	D_p (m ² /s)	D_{AB} (m ² /s)	D_K (m ² /g) ($r = 260 \text{ \AA}$)	t
Helium–ethylene	1.7×10^{-6}	4.82×10^{-5}	8.2×10^{-6}	2.4
Helium–acetic acid	0.84×10^{-6}	4.52×10^{-5}	5.6×10^{-6}	3.4
Helium–vinyl acetate	0.66×10^{-6}	3.12×10^{-5}	4.1×10^{-6}	3.2

TABLE 7
Overall Mass Transfer Coefficients. Helium–Acetic Acid/Vinyl Acetate
Binary Mixtures

$V \times 10^2$ (m ³ /h)	W_s (g)	$K_A \times 10^3$ (m/s)	$K_V \times 10^3$ (m/s)	Mean deviation (%)
9.02	4.02	6.8	3.8	5.7
7.33	4.02	6.5	3.9	8.9
0.93	4.02	6.7	2.8	7.5
9.07	8.02	6.9	2.5	11.1
6.69	8.02	6.9	2.4	9.3
4.50	8.02	6.7	2.7	12.7

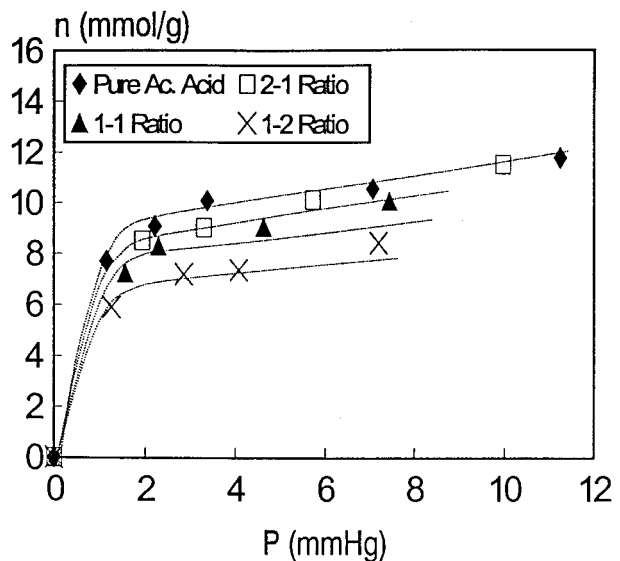
where n_A and n_V are the adsorbed amount of acetic acid and vinyl acetate (mmol/g), respectively, and p_A and p_V are the corresponding partial pressures (mmHg). The fit to Eqs. (22) and (23) is shown in Fig. 6. Average deviations are 1.5 and 9.5% for acetic acid and vinyl acetate, respectively.

Kinetic data have been determined from the model of adsorption with an overall mass transfer coefficient. Two partial mass balances (acetic acid and vinyl acetate) are needed in this case (3). Two global mass coefficients (K_A and K_V) are obtained (Table 7). These coefficients remain practically constant in the range of flows studied.

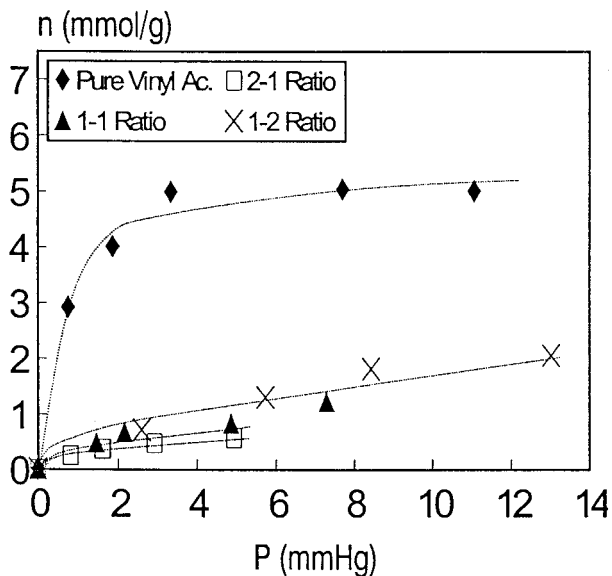
Mass coefficients obtained from binary adsorption are higher than those from pure compounds. For binary mixtures, mass transfer not only occurs from outside to inside the particles, but there is also a displacement of one adsorbate. An example of experimental data and model correlation is shown in Fig. 7.

Equilibrium and kinetic data have been used for the design of an adsorption installation for the removal of acetic acid from the ethylene recycle stream of an industrial plant aimed at treating a flow of 700 kg/h containing 300 ppm of acetic acid and 2140 ppm of vinyl acetate at a pressure of 1.5 kg/cm² (3). The





a)



b)

FIG. 6 Binary mixture adsorption equilibrium data. a): Isotherm for adsorption of acetic acid on activated carbon. Adjustment of experimental data to Eq. (22). Helium-acetic acid-vinyl acetate system. b): Isotherm for adsorption of vinyl acetate on activated carbon. Adjustment of experimental data to Eq. (23). Helium-acetic acid-vinyl acetate system.



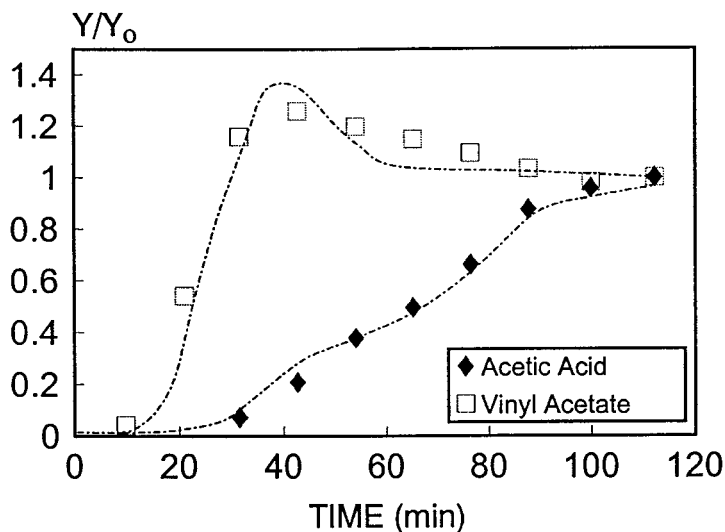


FIG. 7 Binary mixture adsorption kinetics. Adsorption data of helium–acetic acid–vinyl acetate mixtures. Correlation to adsorption model with overall mass transfer coefficients (---).

installation consists of two adsorption columns working alternatively on adsorption and regeneration cycles. Temperature at the bed inlet is 20°C. A bed of 1.23 m diameter and 2.70 m height filled with 1090 kg of adsorbent (activated carbon) was found to be necessary with an operation cycle time of 94.2 hours. Regeneration conditions were 498 K for 48 hours under a nitrogen stream of 327 N·m³/h.

ACKNOWLEDGMENT

The authors thank Repsol Química S.A. for financial support of this research.

REFERENCES

1. J. Collado, *Ing. Quím.*, p. 103 (1989).
2. *Ullman's Encyclopedia of Industrial Chemistry*, 5th ed., VCH Publishers, New York, NY, 1989.
3. A. Sánchez, Ph.D. Thesis, Universidad Complutense, Madrid, 1996.
4. A. De Lucas, G. Ovejero, and A. Sánchez, *Sep. Sci. Technol.*, 27, 1197–1210 (1992).
5. S. Shivaji, *Fundamentals of Adsorption*, Kodansha, Tokyo, 1992.
6. R. B. Eldridge, *Ind. Eng. Chem. Res.*, 32, 2208 (1993).
7. M. H. Stenzel, *Chem. Eng. Prog.*, p. 36 (1993).
8. F. Fajula and D. Pleeb, *Adv. Zeolite Sci. Appl.*, 85, 633 (1994).
9. M. Suzuki, *Chemical Engineering Monograph 25*, Kodansha, Tokyo, 1990.
10. W. J. Thomas and J. L. Lombardi, *Trans. Inst. Chem. Eng.*, 49, 240 (1971).



11. E. Costa, A. De Lucas, and M. A. González, *Ind. Eng. Chem., Fundam.*, 23, 400–405 (1984).
12. D. Do and R. Rice, *Chem. Eng. Sci.*, 42, 2269 (1987).
13. N. Wakao and T. Funazkri, *Ibid.*, 33, 1375 (1978).
14. M. F. Edwards and J. F. Richardson, *Ibid.*, 23, 109 (1993).
15. E. Costa, G. Calleja, and L. Marijuan, *Adsorp. Sci. Technol.*, 5, 213 (1988).
16. E. N. Fuller, P. D. Schettler, and J. C. Giddings, *Ind. Eng. Chem.*, 58, 18 (1966).
17. W. Fritz and E. V. Schlünder, *Chem. Eng. Sci.*, 36, 771 (1981).

Received by editor December 31, 1997

First revision received March 1998

Second revision received May 1998





PAGE 544 IS BLANK



Request Permission or Order Reprints Instantly!

Interested in copying and sharing this article? In most cases, U.S. Copyright Law requires that you get permission from the article's rightsholder before using copyrighted content.

All information and materials found in this article, including but not limited to text, trademarks, patents, logos, graphics and images (the "Materials"), are the copyrighted works and other forms of intellectual property of Marcel Dekker, Inc., or its licensors. All rights not expressly granted are reserved.

Get permission to lawfully reproduce and distribute the Materials or order reprints quickly and painlessly. Simply click on the "Request Permission/Reprints Here" link below and follow the instructions. Visit the [U.S. Copyright Office](#) for information on Fair Use limitations of U.S. copyright law. Please refer to The Association of American Publishers' (AAP) website for guidelines on [Fair Use in the Classroom](#).

The Materials are for your personal use only and cannot be reformatted, reposted, resold or distributed by electronic means or otherwise without permission from Marcel Dekker, Inc. Marcel Dekker, Inc. grants you the limited right to display the Materials only on your personal computer or personal wireless device, and to copy and download single copies of such Materials provided that any copyright, trademark or other notice appearing on such Materials is also retained by, displayed, copied or downloaded as part of the Materials and is not removed or obscured, and provided you do not edit, modify, alter or enhance the Materials. Please refer to our [Website User Agreement](#) for more details.

Order now!

Reprints of this article can also be ordered at
<http://www.dekker.com/servlet/product/DOI/101081SS100100664>